Mass spectrometric characterization of intact desferal-conjugated monoclonal antibodies for immuno-positron emission tomography imaging

Mass spectrometric characterization of intact desferal-conjugated monoclonal antibodies for immuno-PET imaging.

Thomas De Vijlder[1*], Jens Fissers[2,3], Bianca Van Broeck[4], Leonie wyffels[2,5], Marc Mercken[4] and Darrel J Pemberton[6]

1. Pharmaceutical Development & Manufacturing Sciences, Janssen Research & Development, Janssen Pharmaceutica NV, Beerse, Belgium

2. Molecular Imaging Center Antwerp, University of Antwerp, Antwerp, Belgium

3. Laboratory of Medicinal Chemistry, University of Antwerp, Antwerp, Belgium

4. Neuroscience Discovery, Janssen Research & Development, Janssen Pharmaceutica NV, Beerse, Belgium

5. Department of Nuclear Medicine, University Hospital Antwerp, Edegem, Belgium

6. Neuroscience Experimental Medicine, Janssen Pharmaceutica NV, Beerse, Belgium

*Corresponding author: Thomas De Vijlder, tdevijld@its.jnj.com, +32 14602554

Short title:

Intact analysis of chelator-conjugated antibodies

Keywords:

Immuno-PET, monoclonal antibodies, intact mass analysis, Alzheimer's disease

This article has been accepted for publication and undergone full peer review but has not been through the copyediting, typesetting, pagination and proofreading process which may lead to differences between this version and the Version of Record. Please cite this article as doi: 10.1002/rcm.8209

Abstract

Rationale

Immuno-PET imaging may prove to be a diagnostic and progression/intervention biomarker for Alzheimer's disease (AD) with improved sensitivity and specificity. Immuno-PET imaging is based on the coupling of an antibody with a chelator that captures a radioisotope thus serving as an in-vivo PET ligand. A robust and quality controlled process for linking the chelator to the-antibody is fundamental for the success of this approach .

Methods

The structural integrities of two monoclonal antibodies (trastuzumab and JRF/AβN/25) and the quantity of desferal-based chelator attached following modification of the antibodies were assessed by online desalting and intact mass analysis. Enzymatic steps for the deglycosylation and removal of C-terminal lysine was performed sequentially and in a single tube to improve intact mass data.

Results

Intact mass analysis demonstrated that inclusion of enzymatic processing was critical to correctly derive the quantity of chelator linked to the monoclonal antibodies. For trastuzumab, enzymatic cleaving of the glycans was sufficient, whilst additional removal of the C-terminal lysine was necessary for JRF/AβN/25 to ensure reproducible assessment of the relatively low amount of attached chelator.

Conclusions

An efficient intact mass analysis-based process was developed to reproducibly determine the integrity of monoclonal antibodies and the quantity of attached chelator. This technique could serve as an essential quality control approach for the development and production of immuno-PET tracers.

Introduction

Late onset Alzheimer's disease (AD) is the most prevalent cause of dementia in the elderly and it is one of the most challenging diseases of modern society. This neurodegenerative disorder is at present incurable and difficult to diagnose at the very early stages of the disease. Currently, diagnosis is typically dependent on behavioral measures, predominantly observation of impaired cognition and/or memory loss that only becomes apparent during the later stages of AD. As novel treatment approaches are now directed at the earlier stages of AD because these are more likely to lead to improved outcomes, there is a clear and urgent need for improved diagnostic tools and biomarkers.

Together with magnetic resonance imaging (MRI) and protein biomarker detection in cerebrospinal fluid, positron emission tomography (PET) is the most utilized and promising technique for the non-invasive diagnosis of AD in an earlier stage [1]. PET imaging typically uses small molecules or proteins that contain or are labeled with a positron emitting radionuclide. Recently, immuno-PET imaging approaches where radiolabeled monoclonal antibodies (mAbs) are used as radiotracers have emerged as an interesting research tool, particularly in oncology [2]. Importantly, several research groups have also explored immuno-PET tracers for imaging disease progression in mouse models of AD [3] [4] [5] .

We have recently developed an immuno-PET tracer based on JRF/AβN/25, a mAb directed against amyloid β (Aβ) $_{1-x}$ peptide that recognizes an epitope in the first seven residues of Aβ [6][7]. We showed that the JRF/AβN/25-based tracer was able to penetrate the blood-brain-barrier and detect Aβ plaques in the APPPS1-21 transgenic mouse model *in vivo* [8][9]. In these studies, Zirconium-89 (^{89}Zr) was used as radioisotope and this was complexed to the mAb after conjugation with a bifunctional chelator, p -isothiocyanatobenzyl-desferrioxamine (Df-Bz-NCS, further referred to as desferal), as previously optimized by Vosjan and colleagues [10][11]. Desferal is selectively attached to lysine side chain amines via a reaction with the isothiocyanate moiety. The attached desferal molecule can then act as a chelator to complex ^{89}Zr (Figure 1). In addition to its diagnostic utility, immuno-PET approaches that use ^{89}Zr-desferal can also be employed to probe pharmacokinetic (PK) properties and assess tumor targeting of novel compounds in oncology [12] [13].

The assessment of the integrity of an antibody-chelator conjugate (ACC) and the chelator-to-antibody ratio (CAR) is a pivotal quality control step prior to labelling the conjugate with ^{89}Zr. For desferal-conjugated mAbs, the chelate number is usually determined using a radiometric isotopic dilution assay[14]. This method is however time consuming and typically consumes over 1 mg of conjugated-mAb, which can make this approach prohibitively costly for research specific mAbs.

In this study, we describe a straightforward intact mass analysis based approach and demonstrate that intact mass analyses combined with enzymatic treatment to reduce antibody complexity can reproducibly quantify CARs, even when only low amounts of drug or chelator are attached. The strategy is analogous to that used to estimate drug-to-antibody ratio (DAR) on lysine-linked antibody-drug-conjugates (ADCs), which are an important emerging class of therapeutic molecules, especially in oncology [15] [16]. The different analytical methods to characterize ADCs are the subject of several reviews [17] [18].

ACCs and ADCs can be highly complex molecules due to the superposition of the heterogeneity in the number of conjugated molecules and the inherent variability that is characteristic to mAbs [19]. Therefore, sample preparation becomes of pivotal importance and occasionally additional enzymatic steps for the deglycosylation and removal of C-terminal lysine are necessary to deconvolute the obtained mass spectra. We show that this especially holds true for research-type antibodies such as JRF/AβN/25, in which the production and homogeneity is less tightly controlled compared to mAbs that are under clinical assessment.

Experimental procedures

Chemicals & reagents

The JRF/AβN/25 mAb directed against $A\beta_{1-x}$ was developed by Janssen Pharmaceutica NV (Beerse, Belgium). Df-Bz-NCS (desferal) was obtained from Macrocyclics (Dallas, TX, USA). trastuzumab was purchased from Roche (Basel, Switzerland). PNGase F enzyme was purchased from Promega (Leiden, The Netherlands), whilst Carboxypeptidase B (CPB) was obtained from Roche Life Science (Vilvoorde, Belgium). Formic acid was acquired from Merck (Overijse, Belgium) and all other chemicals were purchased from Sigma-Aldrich (Beerse, Belgium). All chemicals were of analytical grade or higher.

Desferal conjugation

Conjugation of desferal was executed as previously described [8]. Briefly, an aqueous solution of 500 µL of antibody at 4 mg/mL was diluted to 970 µL with saline, adjusted to pH 9 using 0.1 M Na_2CO_3, and mixed with a six-fold excess of Df-Bz-NCS (5mM, 17 µL in DMSO). The reaction mixture was

stirred at 550 rpm for 30 min at 37°C. Subsequently, remaining unreacted Df-Bz-NCS was removed using a PD-10 desalting column (GE Healthcare Life Sciences, Diegem, Belgium) that was eluted with 0.25 M sodium acetate buffer (pH 4.9–5.3).

Centrifugal filtration

A buffer exchange step was performed on the desferal conjugated mAb solutions containing 0.25 M sodium acetate. For this, vivaspin 500 filters (GE Healthcare Life Sciences) with a molecular weight cut-off (MWCO) of 10 kDa were used for centrifugal filtration. 50 µL of an antibody solution of 1 mg/mL was centrifuged at 10 000 g for 10 min at 4°C. Afterwards, 450 µL of 50 mM ammonium bicarbonate was added to remove the non-volatile salts. This was followed by an additional centrifugation step. This procedure was repeated four times for a total of five washing steps. Finally, 50 mM ammonium bicarbonate was added to obtain a final antibody concentration of approximately 0.5 mg/mL.

Enzymatic deglycosylation and removal of C-terminal lysines

Enzymatic treatments were performed sequentially and in a single tube. Deglycosylation was accomplished via hydrolysis by PNGase F. Following centrifugal filtration, 15 µL of PNGase was added to the antibodies in 50 mM ammonium bicarbonate (pH 8), followed by incubation at 37°C for 6h (corresponding to 150 units PNGase for 0.05 mg of antibody). Subsequently, samples were analyzed by LC-MS or advanced for the removal of C-terminal lysines through treatment with CPB. For this, 3 µL of CPB (corresponding to 1.2 units for 0.05 mg of antibody) was added to the deglycosylated antibodies and incubated at 25°C for 1h. Treated antibodies were then immediately used for LC-MS analysis or stored at -70°C until analysis.

Enzymatic digestion of antibodies with trypsin

Trypsin digestion was performed on 100 µg Df-Bz-NCS-conjugated JRF/AβN/25 antibody preparations, both prior to, and after enzymatic deglycosylation and C-terminal lysine removal. A centrifugal filtration step at 10 kDa MWCO was performed to a denaturation buffer containing 6 M urea and 2 M thiourea in 50 mM ammonium bicarbonate (pH 7.5) at volume of 100 µL. 10 mM dithiotreitol (DTT) was added to reduce disulfide bonds at 37°C for 1h. Free cysteine residues were alkylated with 20 mM iodoacetamide at room temperature in the dark for 1h. Afterwards, 20mM DTT was added to quench the alkylation reaction. The samples were diluted by addition of 700 µL 50 mM ammonium bicarbonate. An amount of 15 µg sequencing-grade trypsin was added and incubated

overnight at 37°C for proteolysis. The proteolysis was quenched by adding formic acid to a concentration of 1% (v/v).

Intact mass analysis.

Desferal-conjugated mAbs with or without enzymatic treatment were subjected to intact mass analysis. Ten microliters of mAb solution (approximately 1 mg/mL) in 50 mM ammonium bicarbonate (pH 8) were injected in to a H-Class UPLC system (Waters) equipped with a MassPREP micro desalting column for online desalting. The mAbs were eluted from the column by a linear gradient from 100% mobile phase A (0.1% (v/v) formic acid in water) to 100% mobile phase B (0.1% (v/v) formic acid in acetonitrile) over 4 min. A flow rate of 0.2 mL/min was used. A quadrupole time-of-flight mass spectrometer (Synapt G2 HDMS, Waters) was interfaced with the chromatographic system via an electrospray ionization source operating in positive ion mode. An electrospray capillary voltage of 3.2 kV and a sample cone voltage of 80 V were applied. A source temperature and desolvation temperature of 120°C and 450°C were used, respectively. A cone gas flow of 20 L/h and desolvation gas flow of 800 L/h were applied. Mass spectra were recorded over a mass range of 700 to 4000 m/z and in "sensitivity" mode.

Liquid chromatography-tandem mass spectrometry of enzymatically digested antibodies.

Antibody digests were analyzed on a Q Exactive Plus Orbitrap mass spectrometer (Thermo Scientific, Bremen, Germany). An Ultimate 3000 UHPLC system (Thermo Scientific), A 2.1 x 150 mm CSH (130Å, 1.7 µm particle size) column (Waters) was used for separation of the tryptic peptides. Mobile phase A was 0.1% (v/v) formic acid in water, while mobile phase B was 0.1% formic acid (v/v) in acetonitrile. The peptides were eluted with a 107-min gradient (hold at 0% B for 5 min, 0-14.5% B in 50 min, 14.5-50% B in 57 min) at a flow rate of 0.3 mL/min. The mass spectrometer was operated in positive ion mode with a precursor ion scan with a mass range of *m/z* 200-2000 at a resolving power of 70 000 (*m/z* 200). The 8 most abundant multiply charged ions reaching an intensity threshold of 8 e^4 from each precursor ion scan were selected for a product ion scan with higher-energy collision-induced dissociation (HCD) at a resolving power of 17 500 (*m/z* 200) using an NCE of 28. The ESI source voltage was set at 3.6 kV, and the capillary temperature was set at 320°C.

Data analysis

Combined mass spectra from intact mass analysis were deconvoluted via the MaxEnt I algorithm (Waters). The output mass range was 142 to 147 kDa with a resolution of 1 Da/channel. Based on the obtained intact mass spectra and comparison with mock spectra, the minimum intensity ratios were set to 80% and the uniform Gaussian model was applied with a 2 Da width at median height. The MaxEnt I algorithms was used from the Masslynx version 4.1 software platform or within the Biopharmalynx 2.1 software (Waters). The distribution of desferal (as a percentage) was calculated by dividing the peak areas for a particular mAb species by the sum of the peak areas for all species (unlabeled and labeled). Subsequently, the CAR was determined by summing the chelator load distributions (%) multiplied with their corresponding chelator load (i.e. the number of bound chelator molecules) [20].

Results and Discussion

Intact mass analysis of desferal-conjugated trastuzumab

The ACCs assessed here were generated by conjugating Df-Bz-NCS to the monoclonal antibody via a nucleophilic addition reaction to the amino-termini and ε-amine of lysines (Figure 1). In a second step, the modified mAb could then be labeled with ^{89}Zr by binding of the isotope to the desferal moiety. First, intact mass analysis was applied to desferal-labeled trastuzumab. This thoroughly characterized monoclonal antibody was used to optimize the conjugation procedure and the instrument settings such as cone voltage (80 V) and source pressure. Following optimization, no dissociation of the heavy chain or light chain or other smaller antibody fragments was observed in the spectrum. Also, no ions in the lower m/z range corresponding to in-source fragmentation of desferal were detected under the applied conditions, whilst these appeared under harsher ionization conditions, for example when a higher cone voltage was applied. The MassPREP column was used in conjunction with a very short, 4-min gradient to ensure proper desalting of the samples and did not induce separation of the different mAb species. This way, quantification of the CAR will not be influenced by differences in ionization efficiencies that might result from altered mobile phase composition during elution.

For desferal-conjugated trastuzumab, a clear charge state distribution was observed from m/z 2500 to m/z 3500, approximately (Figure 2(A)). The most intense charge states appeared between +49 (m/z 3020-3050) and +48 (m/z 3085-3115).

When zooming in on a single charge state (+48) (Figure 2(B)), a fine structure corresponding to the different glycosylation forms and the desferal-labeling could be distinguished. Following deconvolution of the intact mass spectrum by the MaxEnt I algorithm (Figure 2(C)), a complex pattern of (desferal-conjugated) trastuzumab isoforms is apparent. The observed pattern in Figure 2(C) is caused by the superimposed heterogeneities of the different glycosylation forms and the number of desferal molecules attached to a single trastuzumab protein. The most abundant glycoforms of the unconjugated (0x Df-Bz), singly (1x Df-Bz)- and doubly (2x Df-Bz)-conjugated trastuzumab species are annotated in figure 2(C). The obtained masses and mass errors for the most prominent species are listed in Table 1. Most mass accuracies were below 100 ppm and similar to those reported prior on similar instrumentation [21][22]. The major glycoforms of unconjugated trastuzumab that were observed (Figure 2(C)), and their respective ratios corresponded well to those reported by others {20}. It was noted that minor mAb species that contain one or two desferal molecules can show a larger mass deviation. This was also observed by others before [23] and may be caused by the superposition of multiple species with similar masses (e.g. containing different glycans or a different number of desferal molecules). Moreover, this also may be since these doubly conjugated (2x Df-Bz) species are of lower intensity in our analyses (Figure 2(C)), hampering accurate deconvolution of the intact mass spectra. When available, the use of higher resolution instruments based on orbitrap or FTICR technology may facilitate interpretation and reduce errors caused by deconvolution of the spectra [24]. The complexity of the pattern observed in Figure 2(C) however hampers a simple deduction of the CAR. One frequently applied approach to reduce the heterogeneity of mAb intact mass spectra is the use of specific deglycosylation enzymes such as N-glycosidase (PNGase F) [25]. Following deglycosylation with this enzyme, which essentially cleaves between the lysine residue and the first GlcNac residue of most complex carbohydrates, the deconvoluted intact mass spectrum was simpler to interpret (Figure 2(D)) and the chelator distribution was be easily observed.

Intact mass analysis of desferal-conjugated JRF/AβN/25

The optimized intact mass analysis procedure was then applied to the JRF/AβN/25 research tool antibody directed against $A\beta_{1-x.}$ From the deconvoluted intact mass spectra (Figure 3(A)), no meaningful information regarding the conjugation could be extracted and no conclusions on the CAR could be deduced. As shown in Figure 3(B), following PNGase F treatment, the complexity of the deconvoluted intact mass spectrum was reduced and the peaks in the deconvoluted mass spectrum became more pronounced. The major peaks observed in Figure 3(B) shifted to a lower mass by approximately 3 kDa compared to the major peak prior to PNGase f treatment (figure 3(A)). This corresponds to the loss of two fucosylated diantennary oligosaccharide structures such as G0F, G1F and/or G2F, that are typically observed in IgGs [26]. The three most abundant species in Figure 3(B)

were detected with mass increments of approximately 128 Da and could be detected at 143175 Da, 143305 Da and 143440 Da, respectively. In the higher mass region, the peaks with a mass corresponding to singly desferal-conjugated JRF/AβN/25 species displayed similar 128 Da mass increments. These mass shifts are caused by the variability in the presence of C-terminal lysine on the heavy chains of the mAbs. In marketed therapeutic mAbs and ADCs or those used in clinical studies, removal of C-terminal lysine is often an integral part of the manufacturing process. Although the sequence of trastuzumab in DrugBank [27] (accession number: DB00072, accessed 01 December 2017) describes the C-terminal lysines on the heavy chain, the actual amount C-terminal lysine is generally <1%, due to the action of basic carboxypeptidases during cell culture [28]. For "research-type" antibodies such as JRF/AβN/25, the quantity and number of C-terminal lysines present on the heavy chains is unknown and may elicit additional heterogeneity of the ACC. Thus, a second enzymatic treatment with CPB was performed to remove the C-terminal lysines prior to intact mass analysis. This was immediately conducted following PNGase treatment in a single tube. This efficient approach also warranted that intact mass analysis could be performed without enzyme removal and this had no impact on the obtained deconvoluted intact mass spectra. This resulted in a simple, single tube, process that did not require additional work-up, which should be beneficial for reproducibility and reduced the sample preparation time.

The CAR can be easily deducted from the deconvoluted intact mass spectrum following enzymatic treatment (Figure 3(C)). In this spectrum, a major peak at 143173 Da was observed, that corresponds to the JRF/AβN/25 mAb without C-terminal lysines on the heavy chains. Another peak at 143927 Da was apparent in figure 3(C). This peak displays a mass increment of 754 Da, which closely approximates that of a single desferal conjugation (+ 752 Da) to the JRF/AβN/25 antibody. Another, minor, peak could be detected for the doubly desferal-conjugated JRF/AβN/25 at 144677 Da.

One could hypothesize that a desferal label, conjugated to the C-terminal lysine could either impair CPB treatment or cause cleavage of desferal-conjugated lysine. The latter would cause an underestimation of the observed CAR. Therefore, trypsin digestion and LC-MS/MS -based peptide mapping was applied to investigate the presence of desferal on the C-terminal lysine. The digested peptide containing the carboxy-terminus of the heavy chain of desferal conjugated JRF/AβN/25 was identified both with (top spectrum in Figure 4and without (bottom spectrum in figure 4) C-terminal lysine. While the fragmentation pattern changed profoundly in the latter, due to the lack of the positively charged C-terminal lysine, b- and y-ions as well as internal fragments could be identified. As expected, the C-terminal peptide containing lysine disappeared upon enzymatic CPB treatment, further proving its efficacy (see supplementary Figure S1). In neither of these samples, a desferal-

conjugated C-terminal peptide could not be detected. This demonstrates that the C-terminal lysine of the heavy chain is not a major desferal conjugation site in JRF/AβN/25.Furthermore, in case the presence of desferal at the C-terminal lysine would impair enzymatic cleavage by CPB, this would also result in an increased peak at 128 Da higher compared to the peak for the singly desferal-conjugated antibody (Figure 3(C)), which was not detected.

Quantification & Calculation of CAR.

Based on the results described above, quantitative estimations on the chelator load distribution and CAR for both ACCs were established (Table 2). For desferal-conjugated trastuzumab, the sample preparation (buffer exchange, deglycosylation) and LC-MS was performed in triplicate from the same desferal-conjugation experiment. This resulted in residual standard deviations (RSD) that were approximately <20%. To assess the repeatability of the LC-MS analysis and MaxEnt 1 deconvolution procedure, 3 replicate injections from the same sample preparation of desferal conjugated JRF/AβN/25 were performed. These were executed on a new, freshly prepared batch of desferal conjugated JRF/AβN/25, immediately frozen after desferal-conjugation and work-up. This resulted in an RSD that was substantially <10%, thus demonstrating that the optimized procedure can be employed to assess the CAR of immuno-PET labeled mAbs in a reproducible manner. At first glance, the determined CAR appears similar for both conjugated trastuzumab (0.34) and conjugated JRF/AβN/25 (0.27). Nevertheless, there is a remarkable difference in the loading distribution between both conjugated antibodies; While the majority of the conjugated trastuzumab contains a single desferal molecule, a clearly larger fraction of JRF/AβN/25 was doubly conjugated (Table 2). The reason for this is unknown, but one might speculate that this could be due to the presence of an additional solvent-exposed lysine in the sequence of JRF/AβN/25. The obtained CAR for the desferal conjugated mAbs is comparable to what has previously been described for desferal-modified mAbs using an isotopic dilution assay [10].

Conclusions

In conclusion, we have established a robust and straightforwardly implementable protocol to determine the amount of desferal that is conjugated to monoclonal antibodies. This includes a serial combination of two enzymatic treatments, PNGase F and carboxypeptidase B, in a single tube with no additional work-up required. This resulted in an intact mass analysis methodology that is applicable to "research-type" antibodies of which the glycosylation pattern and c-terminal lysine content are typically not tightly controlled. The described method reproducibly determined the CAR, even at relatively low conjugation levels. Furthermore, the described approach facilitates a straightforward

quality control check of desferal-conjugated antibodies that are to be used in the development of immuno-PET tracers.

References

1. Scheltens P, Blennow K, Breteler MMB, et al. Alzheimer's disease. *Lancet* 2016;388(10043):505-517. doi: 10.1016/S0140-6736(15)01124-1.
2. Wright BD, Lapi SE. Designing the magic bullet? The advancement of immuno-PET into clinical use. *J. Nucl. Med.* 2013;54(8):1171-1174. doi: 10.2967/jnumed.113.126086
3. Yu YJ, Zhang Y, Kenrick M, et al. Boosting brain uptake of a therapeutic antibody by reducing its affinity for a transcytosis target. *Sci. Transl. Med.* 2011;*3*(84):84ra44. doi: 10.1126/scitranslmed.3002230
4. Magnusson K, Sehlin D, Syvänen S, et al. Specific uptake of an amyloid-β protofibril-binding antibody-tracer in AβPP transgenic mouse brain. *J. Alzheimers Dis* 2013;37(1):29-40. doi: 10.3233/JAD-13002
5. D. Sehlin D, Fang XT, Cato L, Antoni G, Lannfelt L, Syvänen S. Antibody-based PET imaging of amyloid beta in mouse models of Alzheimer's disease. *Nat. Commun.* 2016, 7, 10759. doi: 10.1038/ncomms10759
6. Vandermeeren M, Geraerts M, Pype S, Dillen L, Van Hove C, Mercken M. The functional gamma-secretase inhibitor prevents production of amyloid beta 1-34 in human and murine cell lines. *Neurosci. Lett.* 2001; 315(3):145-148
7. Mathews PM, Jiang Y, Schmidt SD, Grbovic OM, Mercken M, Nixon RA. Calpain activity regulates the cell surface distribution of amyloid precursor protein. Inhibition of calpains enhances endosomal generation of beta-cleaved C-terminal APP fragments. *J. Biol. Chem.* 2002; 277(39):36415-36424. doi: 10.1074/jbc.M205208200
8. Fissers J, Waldron AM, De Vijlder T et al. Synthesis and Evaluation of a Zr-89-Labeled Monoclonal Antibody for Immuno-PET Imaging of Amyloid-β Deposition in the Brain. *Mol. Imaging Biol.* 2016;18(4):598-605. doi: 10.1007/s11307-016-0935-z
9. Waldron AM, Fissers J, Van Eetveldt A, et al. In Vivo Amyloid-β Imaging in the APPPS1-21 Transgenic Mouse Model with a (89)Zr-Labeled Monoclonal Antibody. *Front. Aging Neurosci.* 2016;8:67. doi: 10.3389/fnagi.2016.00067
10. Vosjan MJWD, Perk LR, Visser GWM, et al. Conjugation and radiolabeling of monoclonal antibodies with zirconium-89 for PET imaging using the bifunctional chelate p-isothiocyanatobenzyl-desferrioxamine. *Nat. Protoc.* 2010:5(4):739-743. doi: 10.1038/nprot.2010.13
11. Perk LR, Vosjan MJWD, Visser GWM, et al. p-Isothiocyanatobenzyl-desferrioxamine: a new bifunctional chelate for facile radiolabeling of monoclonal antibodies with zirconium-89 for immuno-PET imaging. *Eur. J. Nucl. Med. Mol. Imaging* 2010;37(2):250-259. doi: 10.1007/s00259-009-1263-1
12. Jauw YWS, Menke-van der Houven van Oordt CW, Hoekstra OS, et al. Immuno-Positron Emission Tomography with Zirconium-89-Labeled Monoclonal Antibodies in Oncology: What Can We Learn from Initial Clinical Trials? *Front. Pharmacol.* 2016;*7*:131. doi: 10.3389/fphar.2016.00131
13. Sijbrandi NJ, Merkul E, Muns JA, et al. A Novel Platinum(II)-Based Bifunctional ADC Linker Benchmarked Using 89Zr-Desferal and Auristatin F-Conjugated Trastuzumab. *Cancer Res.* 2017;77(2):257-267. doi:10.1158/0008-5472.CAN-16-1900
14. Holland JP, Caldas-Lopes E, Divilov V, et al. Measuring the pharmacodynamic effects of a novel Hsp90 inhibitor on HER2/neu expression in mice using Zr-DFO-trastuzumab. *PloS One* 2010;5(1): e8859. doi:10.1371/journal.pone.0008859
15. Thomas A, Teicher BA, Hassan R. Antibody-drug conjugates for cancer therapy. *Lancet Oncol.* 2016;17(6):e254. doi: 10.1016/S1470-2045(16)30030-4

16. Chari RVJ. Targeted cancer therapy: conferring specificity to cytotoxic drugs. *Acc. Chem. Res.* 2008;41(1):98-107. doi: 10.1021/ar700108g
17. Wakankar A, Chen Y, Gokarn Y, Jacobson FS. Analytical methods for physicochemical characterization of antibody drug conjugates. *mAbs* 2011;3(2):161-172.
18. Huang RYC, Chen G. Characterization of antibody-drug conjugates by mass spectrometry: advances and future trends. *Drug Discov. Today* 2016;21(5):850-855. doi: 10.1016/j.drudis.2016.04.004
19. Beck A, Wagner-Rousset E, Ayoub D, Van Dorsselaer A, Sanglier-Cianférani S. Characterization of therapeutic antibodies and related products. *Anal. Chem.* 2013;*85*(2):715-736. doi: 10.1021/ac3032355
20. Basa L. Drug-to-antibody ratio (DAR) and drug load distribution by LC-ESI-MS. *Methods Mol. Biol.* 2013;1045:285-293. doi: 10.1007/978-1-62703-541-5_18
.21. Damen CWN, Chen W, Chakraborty AB, et al. Electrospray ionization quadrupole ion-mobility time-of-flight mass spectrometry as a tool to distinguish the lot-to-lot heterogeneity in N-glycosylation profile of the therapeutic monoclonal antibody trastuzumab. *J. Am. Soc. Mass Spectrom.* 2009;20(11):2021-2033. doi: 10.1016/j.jasms.2009.07.017
22. Xie H, Chakraborty A, Ahn J, et al. Rapid comparison of a candidate biosimilar to an innovator monoclonal antibody with advanced liquid chromatography and mass spectrometry technologies. *mAbs* 2010;*2*(4):379-394.
23. Luo Q, Chung HH, Borths C, et al. Structural Characterization of a Monoclonal Antibody-Maytansinoid Immunoconjugate. *Anal. Chem.* 2016;88(1):695-702. doi: 10.1021/acs.analchem.5b03709
24. Fornelli L, Damoc E, Thomas PM, et al. Analysis of intact monoclonal antibody IgG1 by electron transfer dissociation Orbitrap FTMS. *Mol. Cell. Proteomics* 2012;11(12):1758-1767. doi: 10.1074/mcp.M112.019620
25. Tarentino AL, Plummer TH. Enzymatic deglycosylation of asparagine-linked glycans: purification, properties, and specificity of oligosaccharide-cleaving enzymes from Flavobacterium meningosepticum. *Methods Enzymol.* 1994;230:44-57.
26. Jefferis R. Glycosylation of recombinant antibody therapeutics. *Biotechnol. Prog.* 2005;21(1):11-16. doi: 10.1021/bp040016j
27. Wishart DS, Feunang YD, Guo AC, et al. DrugBank 5.0: a major update to the DrugBank database for 2018. *Nucleic Acids Res.* 2017;46(D1): D1074-D1082. Doi: 10.1093/nar/gkx1037
28. Harris RJ, Kabakoff B, Macchi FD, et al. Identification of multiple sources of charge heterogeneity in a recombinant antibody. *J. Chromatogr. B. Biomed. Sci. App.* 2001;752(2):233-245.

Table 1 Overview of the obtained masses and mass errors of the main glycoforms of trastuzumab, both with and without the presence of Df-Bz-NCS.

number of chelators	glycoform	measured mass	mass error (Da)	mass error (ppm)
0x Df-Bz	G0F/G0F	148056	0	0
	G0F/G1F	148222	4	25
	G0F/G2F or G1F/G1F	148390	10	65
	G1F/G2F	148549	7	44
1x Df-Bz	G0F/G0F	148823	14	97
	G0F/G1F	148980	9	63
	G0F/G2F or G1F/G1F	149147	14	96
	G1F/G2F	149305	10	69
2x Df-Bz	G0F/G0F	149586	25	168
	G0F/G1F	149740	17	114
	G0F/G2F (or G1F/G1F)	149898	13	86
	G1F/G2F	150054	7	46

Table 2 The amount of Df-Bz-NCS labeled to the antibodies and their respective CAR. The intermediate precision was checked on labeled JRF/AβN/25 (repeated LC-MS injections) and trastuzumab (repeated sample preparation and LC-MS injections)

antibody	chelator	distribution (%)	standard error (%)	RSD (%)
		(n=3, sample preparation + LC-MS replicates)		
trastuzumab	0 x desferal	69.0%	2.8%	7.0%
	1 x desferal	27.9%	2.5%	15.4%
	2 x desferal	3.1%	0.4%	20.9%
	CAR	0.34		
		(n=3, LC-MS replicates)		
JRF/AβN/25	0 x desferal	79.3%	0.8%	1.6%
	1 x desferal	14.6%	0.6%	7.5%
	2 x desferal	6.1%	0.2%	6.0%
	CAR	0.27		

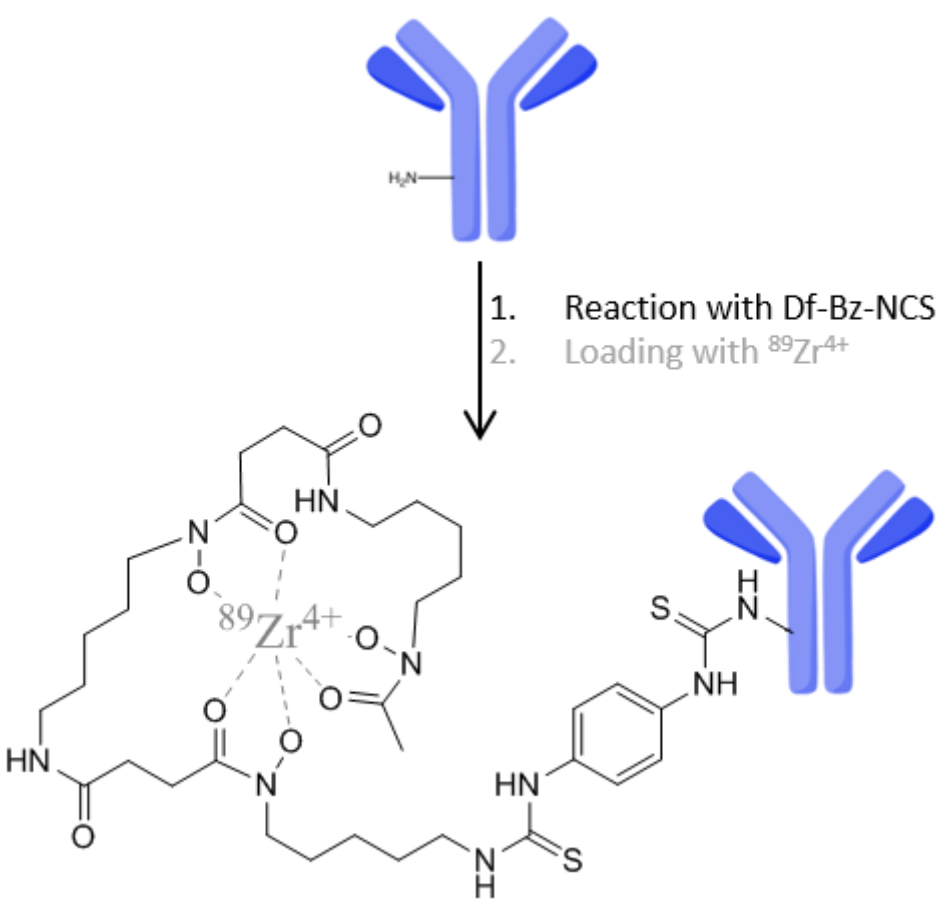

Figure 1 Schematic representation of the chemical structure of Desferal (DF-Bz-NCS) and its conjugation to monoclonal antibodies. LC-MS analyses are performed prior to labeling with $^{89}Zr^{2+}$.

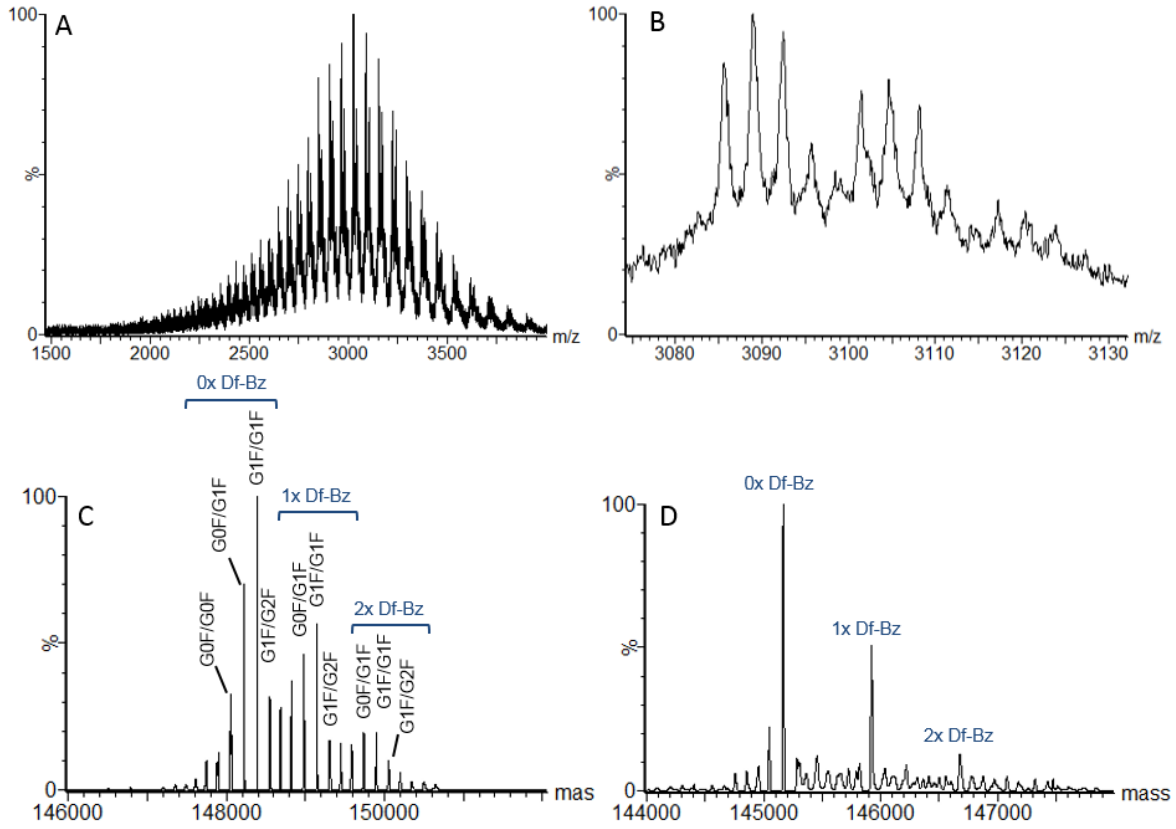

Figure 2 Mass spectra of Df-Bz-NCS conjugated to trastuzumab. (A) Intact mass spectrum. (B) shows a zoom on the +48-charge state. (C) the deconvoluted mass spectrum and, (D) the deconvoluted mass spectrum after deglycosylation by PNGase F. The major species in (C) and (D) are annotated according to their theoretical mass. Df-Bz denotes the number of desferal molecules conjugated. Note that G1F/G1F species also contains G2F/G0F since these species cannot be differentiated by their intact mass.

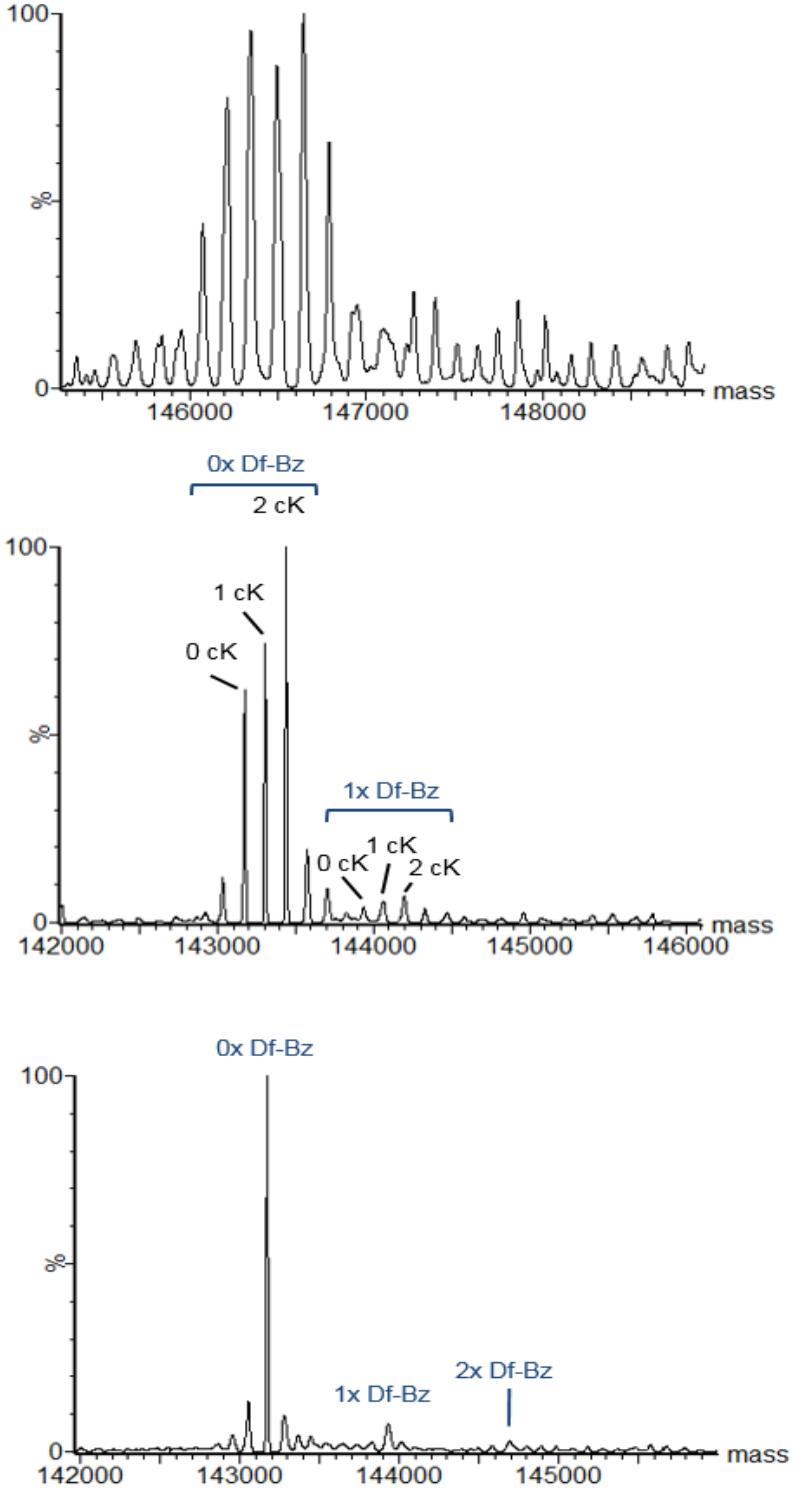

Figure 3 Mass spectra of Df-Bz-NCS conjugated to the JRF/AβN/25 antibody. (A) Deconvoluted mass spectrum. (B) Deconvoluted mass spectrum after deglycosylation by PNGase F. (C) Deconvoluted mass spectrum of the Df-BZ-NCS - JRF/AβN/25 conjugate after one-pot deglycosylation (PNGase F) and C-terminal lysine removal (carboxypeptidase B). cK indicates the number of heavy chain C-terminal lysines present. Df-Bz denotes the number of desferal molecules conjugated.

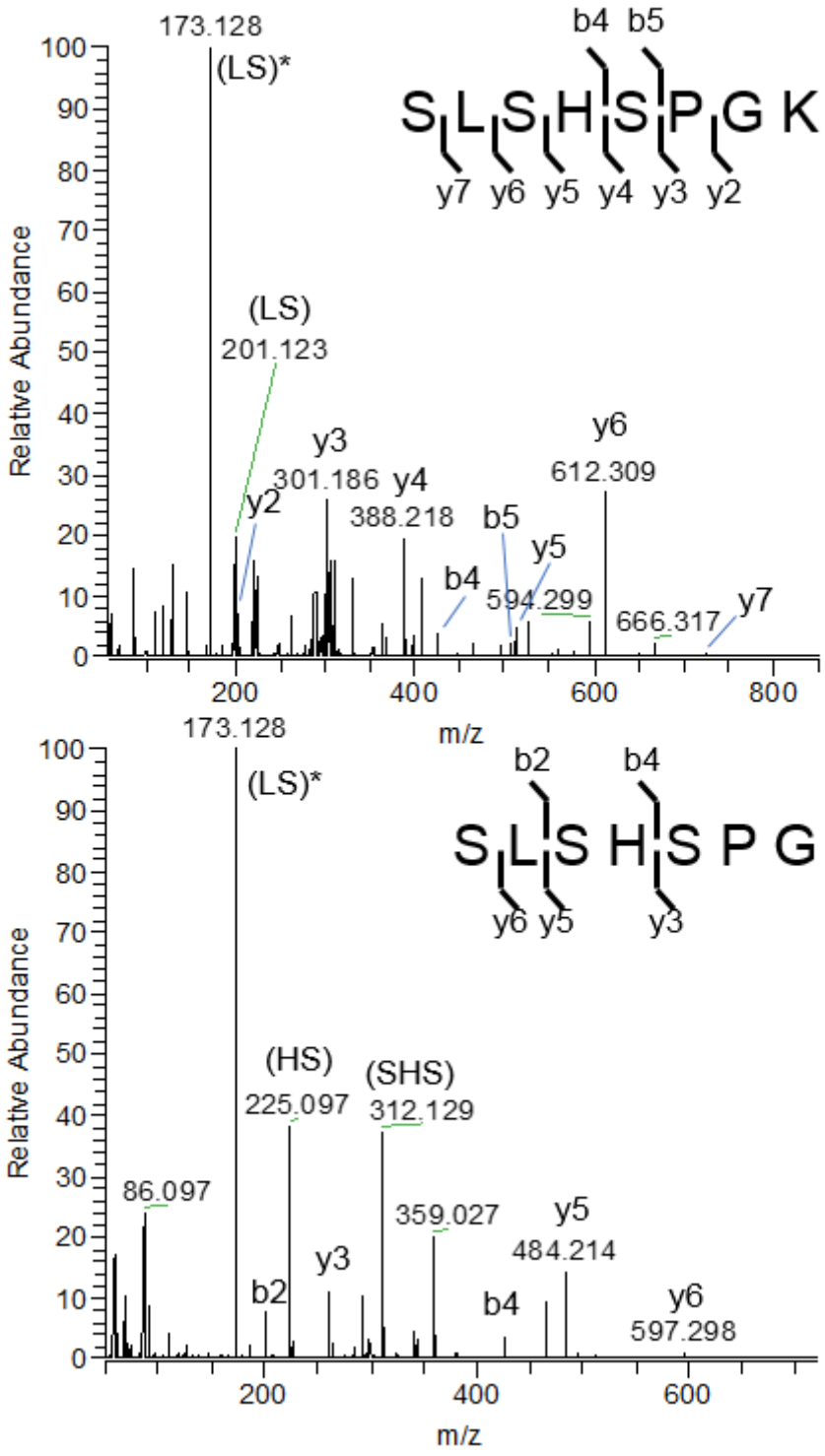

Figure 4: Annotated fragmentation spectra of the carboxyterminal peptide of the heavy chain of Df-Bz-NCS-conjugated JRF/AβN/25, with (top) and without C-terminal lysine (bottom). The annotations in brackets indicate internal product ions, an * denotes the loss of CO (28 Da) from the internal product ions.